Piecewise-Quadratics and Reparameterizations for Interpolating Reduced Data

Ryszard Kozera[1] and Lyle Noakes[2]

[1] Warsaw University of Life Sciences - SGGW
Faculty of Applied Informatics and Mathematics
Nowoursynowska str. 159, 02-776 Warsaw, Poland
[2] Department of Mathematics and Statistics
The University of Western Australia
35 Stirling Highway, Crawley W.A. 6009, Perth, Australia
ryszard_kozera@sggw.pl, lyle.noakes@maths.uwa.edu.au

Abstract. This paper tackles the problem of interpolating reduced data $Q_m = \{q_i\}_{i=0}^m$ obtained by sampling an unknown curve γ in arbitrary euclidean space. The interpolation knots $\mathcal{T}_m = \{t_i\}_{i=0}^m$ satisfying $\gamma(t_i) = q_i$ are assumed to be unknown (*non-parametric interpolation*). Upon selecting a specific numerical scheme $\hat{\gamma}$ (here a *piecewise-quadratic* $\hat{\gamma} = \hat{\gamma}_2$), one needs to supplement Q_m with knots' estimates $\{\hat{t}_i\}_{i=0}^m \approx \{t_i\}_{i=0}^m$. A common choice of $\{\hat{t}_i^{\lambda}\}_{i=0}^m$ ($\lambda \in [0,1]$) frequently used in curve modeling and data fitting (e.g. in computer graphics and vision or in computer aided design) is called *exponential parameterizations* (see, e.g., [11] or [16]). Recent results in [8] and [14] show that $\hat{\gamma}_2$ combined with exponential parameterization yields (in trajectory estimation) either linear $\alpha(\lambda) = 1$ ($\lambda \in [0,1)$) or cubic $\alpha(1) = 3$ convergence orders, once Q_m gets progressively denser. The asymtototics proved in [8] relies on the extra assumptions requiring $\hat{\gamma}_2$ to be reparameterizable to the domain of γ. Indeed, as shown in [14], a natural candidate ψ for such a reparameterization meets this criterion only for $\lambda = 1$, whereas the latter (see [8]) may not hold for the remaining $\lambda \in [0,1)$ (which e.g. brings difficulty in length estimation of γ by using $\hat{\gamma}$). Our paper fills out this gap and establishes sufficient conditions imposed on $\mathcal{T}_m$ to render ψ a genuine reparameterization with $\lambda \in [0,1)$ (see Th. 4). The derivation of a such a condition involves theoretical analysis and symbolic computation, and this constitutes a novel contribution of the present work. The numerical tests verifying whether ψ indeed is a reparameterization (for $\lambda \in [0,1)$ and for more-or-less uniform samplings $\mathcal{T}_m$) are also performed. The sharpness of the asymptotics in question is additionally confirmed with the aid of numerical tests.

1 Introduction

Sampled data points $\gamma(t_i) = q_i$ with $(\{t_i\}_{i=0}^m, Q_m)$ form a pair of a so-called *non-reduced data*. It is required here that $t_i < t_{i+1}$ and $q_i \neq q_{i+1}$ hold. In addition, we assume that $\gamma : [0,T] \to E^n$ (with $0 < T < \infty$) is sufficiently smooth (specified

V.P. Gerdt et al. (Eds.): CASC 2015, LNCS 9301, pp. 260–274, 2015.
DOI: 10.1007/978-3-319-24021-3_20

later) and that it defines a regular curve (i.e. $\dot{\gamma}(t) \neq \mathbf{0}$). In order to approximate the curve γ with an arbitrary interpolant $\bar{\gamma}\colon [0,T] \to E^n$ it is necessary to assume that the knots fulfill the *admissibility condition* (denoted as $\{t_i\}_{i=0}^m \in V_G^m$):

$$\lim_{m\to\infty} \delta_m = 0, \quad \text{where} \quad \delta_m = \max_{0\leq i\leq m-1}(t_{i+1} - t_i). \tag{1}$$

This paper discusses a special subfamily of admissible samplings $V_{mol}^m \subset V_G^m$ called *more-or-less uniform* samplings (see e.g. [7]) defined as:

$$\beta\delta_m \leq t_{i+1} - t_i \leq \delta_m, \tag{2}$$

for some $\beta \in (0,1]$. Note that the left inequality in (2) excludes samplings with distance between consecutive knots smaller than $\beta\delta_m$. On the other hand the right inequality in (2) holds automatically due to (1).

For $\mathcal{T}_m$ unknown, a proper choice of guessed knots $\{\hat{t}_i\}_{i=0}^m \approx \{t_i\}_{i=0}^m$ is stipulated by enforcing the convergence of the selected interpolant $\hat{\gamma}$ (satisfying $\hat{\gamma}(\hat{t}_i) = q_i$) to the unknown curve γ with possibly fast orders. Recall that we choose here $\hat{\gamma} = \hat{\gamma}_2$ as a Lagrange piecewise-quadratic interpolant fitting consecutive triples of points from Q_m. At best the resulting asymptotics in trajectory estimation by any interpolant $\hat{\gamma}$ (and thus in particular by $\hat{\gamma}_2$) should match the asymptotics derived for the corresponding classical *parametric interpolant* $\bar{\gamma}$ (here a piecewise-quadratic $\bar{\gamma} = \tilde{\gamma}_2$) based on non-reduced data $(\{t_i\}_{i=0}^m, Q_m)$, with $\mathcal{T}_m$ specified. The next section outlines the existing results on interpolating reduced data and formulates a research task for this paper (see Th. 4).

2 Problem Formulation and Motivation

Recall that the family $F_{\delta_m}\colon [0,T] \to E^n$ satisfies $F_{\delta_m} = O(\delta_m^\alpha)$ if $\|F_{\delta_m}\| = O(\delta_m^\alpha)$, where $\|\cdot\|$ denotes the euclidean norm and $\alpha \in \mathbb{R}$. By well-known convention, the latter guarantees the existence of constants $K > 0$ and $\bar{\delta} > 0$ (independent on m) such that $\|F_{\delta_m}\| \leq K\delta_m^\alpha$, for all $\delta_m \in (0, \bar{\delta})$.

A standard result for *non-reduced data* $(\{t_i\}_{i=0}^m, Q_m)$ combined with piecewise r-degree polynomial $\bar{\gamma} = \tilde{\gamma}_r$ reads (see e.g. [7] or [1]):

Theorem 1. *Let $\gamma \in C^{r+1}$ be a regular curve $\gamma : [0,T] \to E^n$. Assume that the knot parameters $\{t_i\}_{i=0}^m \in V_G^m$ are given. Then a piecewise r-degree Lagrange polynomial $\tilde{\gamma}_r$ used with $\{t_i\}_{i=0}^m$ known, yields a sharp estimate for the trajectory estimation $\tilde{\gamma}_r = \gamma + O(\delta_m^{r+1})$.*

In particular, piecewise-quadratics $\tilde{\gamma}_2$ or piecewise-cubics $\tilde{\gamma}_3$ render *cubic* or *quartic* orders in Th. 1, respectively. In various applications in computer graphics and vision (e.g. image segmentation or curve modeling), engineering or physics (trajectory estimation) or medical image processing (e.g. in medical diagnosis) a common situation is to deal exclusively with the *reduced data* Q_m (see e.g. [11], [5], [16] or [3]). Any fitting scheme based on Q_m requires, in the first step to determine the respective substitutes $\{\hat{t}_i\}_{i=0}^m$ (i.e. external knots) approximating

somehow the internal knots $\{t_i\}_{i=0}^m$. One particular family of $\{\hat{t}_i\}_{i=0}^m \approx \{t_i\}_{i=0}^m$ commonly used for curve modeling is the so-called *exponential parameterization* (see e.g. [11] or [12]):

$$\hat{t}_0 = 0, \qquad \hat{t}_{i+1} = \hat{t}_i + \|q_{i+1} - q_i\|^\lambda, \tag{3}$$

where $0 \leq \lambda \leq 1$ and $i = 0, 1, \ldots, m-1$. The special cases of $\lambda \in \{1, 0.5, 0\}$, yield the so-called *cumulative chords, centripetal, and blind uniform parameterizations* of external knots, respectively. We denote a piecewise degree-r polynomial based on (3) and Q_m as $\hat{\gamma} = \hat{\gamma}_r : [0, \hat{T}] \to E^n$, where $\hat{T} = \sum_{i=0}^{m-1} \|q_{i+1} - q_i\|^\lambda$. In order to establish the asymptotics in difference between the curve γ and any non-parametric interpolant $\hat{\gamma}$, *a reparameterization* $\psi : [0, T] \to [0, \hat{T}]$ synchronizing both domains of γ and $\hat{\gamma}_r$ is needed. As mentioned above, the case when $\lambda = 0$ transforms (3) into to blind *uniform* guesses (with no regard to the distribution of Q_m) with $\hat{t}_i = i$. For $r = 2$ and $\lambda = 0$ the linear convergence rate (i.e. $\alpha(0) = 1$) in trajectory estimation was originally proved in [15]. A faster convergence follows if $\lambda = 1$ is assumed to (3). This yields the so-called *cumulative chords* (see e.g. [11] or [16]) satisfying $\hat{t}_0 = 0$ and $\hat{t}_{i+1} = \hat{t}_i + \|q_{i+1} - q_i\|$ for $i = 0, 1, \ldots, m-1$. Such a choice of $\{\hat{t}_i\}_{i=0}^m$ incorporates the geometry of Q_m and consequently offers much better approximation orders $\alpha(1)$ (at least for $r = 2, 3$) as opposed to the case of $\lambda = 0$. Indeed the following holds (see [14]):

Theorem 2. *Suppose γ is a regular C^k curve in E^n, where $k \geqslant r + 1$ and $r = 2, 3$ sampled according to (1). Let $\hat{\gamma}_r : [0, \hat{T}] \to E^n$ be the cumulative chord piecewise degree-r interpolant defined by Q_m and (3) with $\lambda = 1$. Then there is a piecewise-C^r reparameterization $\psi : [0, T] \to [0, \hat{T}]$ with $\hat{\gamma}_r \circ \psi = \gamma + O(\delta_m^{r+1})$.*

Visibly, for $r = 2$ and $\lambda = 1$ the order $\alpha(1) = 3$ determined by Th. 2 improves by 2 the order $\alpha(0) = 1$. In addition, at least for $r = 2, 3$ both asymptotics established in Th. 2 (for $\lambda = 1$) and Th. 1 coincide. Recent result in [8] (for $r = 2$) extends the above two special cases of $\alpha(0) = 1$ and $\alpha(1) = 3$ to the entire family of exponential parameterizations (3), i.e. to all $\lambda \in [0, 1]$. As proved in [8], for arbitrary more-or-less uniform samplings (2) combined with (3) any choice of $\lambda \in [0, 1)$ does not improve the asymptotics in γ approximation by $\hat{\gamma}_2$. In fact a linear convergence order $\alpha(\lambda) = 1$ holds for all $\lambda \in [0, 1)$ and $r = 2$:

Theorem 3. *Suppose γ is a regular C^3 curve in E^n sampled more-or-less uniformly (2). Let $\hat{\gamma}_2 : [0, \hat{T}] \to E^n$ be the piecewise-quadratic interpolant defined by Q_m and (3) (with $\lambda \in [0, 1]$). Then for a special candidate of a piecewise-C^∞ reparameterization $\psi : [0, T] \to [0, \hat{T} = \sum_{i=0}^{m-1} \|q_{i+1} - q_i\|^\lambda]$ and $\lambda \in [0, 1)$ we have $\hat{\gamma}_2 \circ \psi = \gamma + O(\delta_m)$. In addition, for either $\{t_i\}_{i=0}^m$ uniform or $\lambda = 1$ and (1), ψ is a piecewise-C^∞ reparameterization for which we have $\hat{\gamma}_2 \circ \psi = \gamma + O(\delta_m^3)$.*

Th. 3 yields an unexpected left-hand side discontinuity in $\alpha(\lambda)$ at $\lambda = 1$. Indeed by Th. 3 the order $\alpha(\lambda) = 1$ (for $\lambda \in [0, 1)$) jumps abruptly to $\alpha(1) = 3$. As demonstrated in [8], opposite to the cumulative chords the natural candidate for a reparametrization, i.e a piecewise-quadratic $\psi = \{\psi_i\}_{i=0}^{m-2}$ with quadratic

$\psi_i : [t_i, t_{i+2}] \to [\hat{t}_i, \hat{t}_{i+2}]$ satisfying $\psi_i(t_{i+j}) = \hat{t}_{i+j}$ (for $j = 0, 1, 2$, see also (3)) may not render an injective function for the remaining $\lambda \in [0, 1)$. Note that $\psi : [0, T] \to [0, \hat{T}]$ invoked in Th. 3 is defined as a track-sum of ψ_i, where $i = 0, 2, 4, \ldots, m-2$. For various applications like e.g. length estimation of the 2D object in medical image processing or correct trajectory tracking it is vital that ψ is a reparameterization. Therefore in this paper, we formulate and substantiate sufficient conditions imposed on samplings $\{t_i\}_{i=0}^m$ to render ψ_i (and thus ψ) a genuine (in fact here a piecewise C^∞) reparameterization.

Note first that any admissible sampling (including a more-or-less uniform one) can be characterized by (for arbitrary m and $0 \le i \le m$):

$$t_{i+1} - t_i = M_{im}\delta_m \quad \text{and} \quad t_{i+2} - t_{i+1} = N_{im}\delta_m, \tag{4}$$

where $0 < M_{im}, N_{im} \le 1$. Our main result (complementing Th. 3) reads as follows:

Theorem 4. *Let the assumptions from Th. 3 hold. Suppose that sampling $\{t_i\}_{i=0}^m$ (see (4)) fulfills both inequalities determined by (12) and (13) for a fixed $\lambda_0 \in [0, 1)$. Then, each quadratic $\psi_i : [t_i, t_{i+2}] \to [\hat{t}_i, \hat{t}_{i+2}]$ is asymptotically (i.e. for sufficiently large m) a reparameterization, with $\{\hat{t}_i\}_{i=0}^m$ defined according to (3). In addition, the latter holds asymptotically for all exponential parameterizations (3) with $\lambda \in [\lambda_0, 1)$. Finally, if β determining a more-or-less uniformity (2) satisfies $\beta > \sqrt{2}-1$, then ψ is asymptotically a reparameterization for all $\lambda \in [0, 1]$.*

In this paper an analytical proof of Th. 4 is given. In addition, both (12) and (13) are interpreted with the aid of symbolic computation in *Mathematica* and geometrical argument. In practice the first condition (12) is not easy to check. Consequently, a stronger condition (16) is proposed, which can easily be checked by symbolic computation. The verification of (16) (as opposed to (12)) is simpler (at least for symbolic computation) and its satisfaction yields both (12) and (13). Again further geometrical insight is given. The entire procedure for determining whether a given ψ is a reparameterization is illustrated in the closing section of this paper. The experimental results (performed in *Mathematica*) of testing this procedure on various samplings and curves are also presented. Finally, the sharpness of the asymptotics derived in Th. 3 is numerically confirmed. Note also that sufficient conditions for ψ to be a reparameterization specified in Th. 4 complement Th. 3.

3 Main Result

Proof. (i) We prove now Th. 4 (by recalling first [8]). Let $\psi_i : [t_i, t_{i+2}] = I_i \to [\hat{t}_i, \hat{t}_{i+2}] = \hat{I}_i$, be the quadratic polynomial satisfying interpolation conditions $\psi_i(t_{i+j}) = \hat{t}_{i+j}$ (for $j = 0, 1, 2$) with $\hat{t}_i$ defined as in (3). The track-sum of $\{\psi_i\}_{i=0}^{m-2}$ (for $i = 0, 2, 4 \ldots m-2$) defines a piecewise-C^∞ mapping $\psi : [0, T] \to [0, \hat{T}]$. The Newton Interpolation Formula (see [1]) over each I_i yields $\psi_i(t) = \psi_i[t_i] + \psi_i[t_i, t_{i+1}](t - t_i) + \psi_i[t_i, t_{i+1}, t_{i+2}](t - t_i)(t - t_{i+1})$, and therefore

$$\psi_i^{(1)}(t) = \psi_i[t_i, t_{i+1}] + (2t - t_{i+1} - t_i)\psi_i[t_i, t_{i+1}, t_{i+2}]. \tag{5}$$

By [8], for more-or-less uniform samplings $\{t_i\}_{i=0}^m \in V_{mol}^m$ we have (for $k = 0, 1$):

$$\psi_i[t_{i+k}, t_{i+k+1}] = (t_{i+k+1} - t_{i+k})^{-1+\lambda} + O((t_{i+k+1} - t_{i+k})^{1+\lambda}),$$

$$\psi_i[t_i, t_{i+1}, t_{i+2}] = \frac{(t_{i+2} - t_{i+1})^{-1+\lambda} - (t_{i+1} - t_i)^{-1+\lambda}}{t_{i+2} - t_i} + O(\delta_m^\lambda). \tag{6}$$

(ii) We pass now to the *main contribution* of this paper (namely, a proof of Th. 4). For ψ_i to be a reparameterization we need $\psi_i^{(1)} > 0$ over I_i. Taking into account that $\psi_i^{(1)}(t)$ is affine, it is sufficient to show that both $\psi_i^{(1)}(t_i) > 0$ and $\psi_i^{(1)}(t_{i+2}) > 0$ hold, asymptotically. In doing so, by (5) we arrive at:

$$\psi_i^{(1)}(t_i) = \psi_i[t_i, t_{i+1}] + (t_i - t_{i+1})\psi_i[t_i, t_{i+1}, t_{i+2}],$$

$$\psi_i^{(1)}(t_{i+2}) = \psi_i[t_i, t_{i+2}] + [(t_{i+2} - t_{i+1}) + (t_{i+2} - t_i)]\psi_i[t_i, t_{i+1}, t_{i+2}]. \tag{7}$$

We find now sufficient condition under which both inequalities $\psi_i^{(1)}(t_i) > 0$ and $\psi_i^{(1)}(t_{i+2}) > 0$ are satisfied asymptotically. By (1), the consecutive knots' differences determined in (4) yield $M_{im} = O(1)$ and $N_{im} = O(1)$ (in fact here $0 < M_{im} \leq 1$ and $0 < N_{im} \leq 1$). Coupling (4) with (6) gives

$$\psi_i[t_i, t_{i+1}] = M_{im}^{-1+\lambda}\delta_m^{-1+\lambda} + O(\delta_m^{1+\lambda}),$$

$$\psi_i[t_{i+1}, t_{i+2}] = N_{im}^{-1+\lambda}\delta_m^{-1+\lambda} + O(\delta_m^{1+\lambda}). \tag{8}$$

Since $0 < M_{im}, N_{im} \leq 1$, we have $M_{im}^\theta = O(1)$ and $N_{im}^\theta = O(1)$ for each $\theta \geq 0$ (here $\theta = 1 + \lambda$). The latter (with $\theta = \lambda$) together with (4), (6), and $0 < (t_{i+j+1} - t_{i+j})(t_{i+2} - t_i) < 1$, for $j = 0, 1$ yield that $\psi_i[t_i, t_{i+1}, t_{i+2}]$

$$= \frac{N_{im}^{-1+\lambda}\delta_m^{-1+\lambda} - M_{im}^{-1+\lambda}\delta_m^{-1+\lambda}}{(M_{im} + N_{im})\delta_m} + \frac{O((t_{i+2} - t_{i+1})^{1+\lambda}) + O((t_{i+2} - t_{i+1})^{1+\lambda})}{t_{i+2} - t_i}$$

$$= \frac{N_{im}^{-1+\lambda}\delta_m^{-1+\lambda} - M_{im}^{-1+\lambda}\delta_m^{-1+\lambda}}{(M_{im} + N_{im})\delta_m} + O(\delta_m^\lambda). \tag{9}$$

Combining (9) with (7), (8), $M_{im} = O(1)$ and $N_{im} = O(1)$ leads to

$$\psi_i^{(1)}(t_i) = \delta_m^{-1+\lambda}\left(M_{im}^{-1+\lambda} - \frac{M_{im}}{M_{im} + N_{im}}(N_{im}^{-1+\lambda} - M_{im}^{-1+\lambda})\right) + O(\delta_m^{1+\lambda}),$$

$$\psi_i^{(1)}(t_{i+2}) = \delta_m^{-1+\lambda}\left(M_{im}^{-1+\lambda} + \left(1 + \frac{N_{im}}{M_{im} + N_{im}}\right)(N_{im}^{-1+\lambda} - M_{im}^{-1+\lambda})\right) + O(\delta_m^{1+\lambda}). \tag{10}$$

In order to ensure now that both $\psi_i^{(1)}(t_i) > 0$ and $\psi_i^{(1)}(t_{i+2}) > 0$ hold asymptotically, it is sufficient to assume *firstly* that:

$$\rho_1(M_{im}, N_{im}) = M_{im}^{-1+\lambda} - \frac{M_{im}}{M_{im} + N_{im}}(N_{im}^{-1+\lambda} - M_{im}^{-1+\lambda}),$$

$$\rho_2(M_{im}, N_{im}) = M_{im}^{-1+\lambda} + \left(1 + \frac{N_{im}}{M_{im} + N_{im}}\right)(N_{im}^{-1+\lambda} - M_{im}^{-1+\lambda}), \quad (11)$$

are positive and *secondly* that there exist constants $\alpha_1 < 2$, $\alpha_2 < 2$, $K_1 > 0$ and $K_2 > 0$ such that asymptotically we have:

$$\rho_1(M_{im}, N_{im}) \geq K_1 \delta_m^{\alpha_1} \quad \text{and} \quad \rho_2(M_{im}, N_{im}) \geq K_2 \delta_m^{\alpha_2}. \quad (12)$$

Condition (12) ensures that asymptotically the slowest components in (10) are of order less than $\lambda + 1$, which combined with the (11) results (for sufficiently large m) in positive derivatives of ψ_i at both ends of each I_i (and thus over entire I_i). As it turns out, the positivity of the expressions in (11) has a simple geometrical interpretation easily verifiable for any specific samplings $\{t_i\}_{i=0}^m$ and $\lambda \in [0, 1)$. Indeed, upon simple algebraic manipulations both inequalities from (11) are reducible to:

$$2 + \frac{N_{im}}{M_{im}} > \left(\frac{N_{im}}{M_{im}}\right)^{-1+\lambda} \quad \text{and} \quad \left(\frac{N_{im}}{M_{im}}\right)^{-1+\lambda} > 1 - \frac{1 + \frac{N_{im}}{M_{im}}}{2\frac{N_{im}}{M_{im}} + 1}. \quad (13)$$

The system of two non-linear inequalities (13) in two independent variables can be solved by *adopting one of two following geometrically driven approaches*:

a) The first method relies on *homogeneous substitution* $x = (N_{im}/M_{im}) > 0$ applied to both inequalities (13) which in turn leads into:

$$f(x) = 2 + x > g(x) = x^{-1+\lambda} \quad \text{and} \quad g(x) > h(x) = 1 - \frac{1 + x}{2x + 1}. \quad (14)$$

Plotting $f(x) > g(x)$ (e.g. in *Mathematica*) yields for each $\lambda \in [0, 1)$ an interval (a_λ, ∞), where $0 < a_\lambda < 1$ (here $f(a_\lambda) = g(a_\lambda)$). Similarly, upon plotting $g(x) > h(x)$ for each $\lambda \in [0, 1)$ we obtain an interval $(0, b_\lambda)$, where $b_\lambda > 1$ (here $g(b_\lambda) = h(b_\lambda)$). Thus a non-empty intersection of (a_λ, ∞) and $(0, b_\lambda)$ renders *an admissible interval* for samplings $\{t_i\}_{i=0}^m$ from (4) with $(N_{im}/M_{im}) \in (a_\lambda, b_\lambda)$ (see Figure 1, when $\lambda = 0.1$ is used). Table 1 (called here *a look-up table*) lists admissible intervals (a_λ, b_λ) (for $\lambda \in [0, 1)$) which are numerically computed by finding the sole roots of either $f(x) - g(x) = 0$ or $g(x) - h(x) = 0$, with the aid of *Mathematica's NSolve* function. Given $\lambda \in [0, 1)$, the existence of at least one pair of intersection points (a_λ, b_λ) results from the Darboux Theorem upon calculating the limits of f, g and h at the ends of the interval $(0, +\infty)$. On the other hand, the uniqueness of (a_λ, b_λ) follows from the strict monotonicity of f, g and h. Of course for $\lambda \in [0, 1)$ we have $a_\lambda < 1$, since $f(1) - g(1) = 2 > 0$ and $\lim_{x \to 0^+}(f(x) - g(x)) = -\infty$.

The next observation inferable from the graphs of f, g and h reads (for $\lambda \in [0, 1)$ as:

$$0 \leq \lambda_1 < \lambda_2 < 1 \quad \text{then} \quad 0 < a_{\lambda_2} < a_{\lambda_1} < 1 \quad \text{and} \quad 1 < b_{\lambda_1} < b_{\lambda_2}. \quad (15)$$

Note that it suffices to substantiate (15) only for a_λ as the other ones follow from the formula $a_\lambda = (1/b_\lambda)$ (hence also $a_\lambda < b_\lambda$) which is easily verifiable upon using

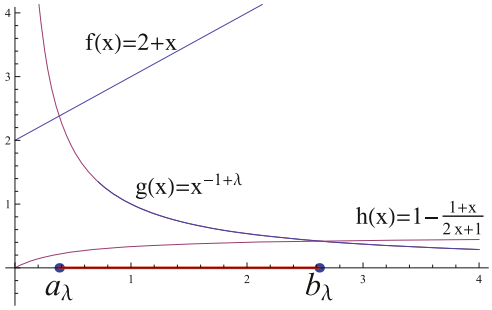

Fig. 1. An admissible interval for $(N_{im}/M_{im}) \in (a_\lambda, b_\lambda) = (0.381, 2.622)$ and $\lambda = 0.1$.

(14). The inequality $a_{\lambda_2} < a_{\lambda_1}$ follows either by an indirect argument or upon resorting to the implicit function theorem. Indeed for the function $i(\lambda, a) = 2 + a - a^{-1+\lambda}$ (with $(\lambda, a) \in [0,1) \times (0, \infty)$), the equation $i(\lambda, a) = 0$ (since $(\partial i/\partial a)(\lambda, a) = 1 + (1-\lambda)a^{-2+\lambda} > 0$ does not vanish) determines $a_\lambda = a(\lambda)$ whose derivative satisfies $a'(\lambda) = (a^{-1+\lambda}\ln(a))/(1 + (1-\lambda)a^{-2+\lambda}) < 0$, as $0 < a < 1$. Thus $a_\lambda = a(\lambda)$ is strictly decreasing. Note also that if $\lambda_n = (1 - c_n) \to 1^-$ (where $c_n \to 0^+$) then $a_{\lambda_n} \to 0^+$. Indeed by monotonicity of a_{λ_n} and $a_{\lambda_n} \geq 0$ the sequence a_{λ_n} is convergent with $\lim_{n\to\infty} a_{\lambda_n} = g \geq 0$. Taking into account (14) we have $2 + a_{\lambda_n} = e^{-c_n \ln(a_{\lambda_n})}$. The latter, if $g \neq 0$ yields $g = -1$, a contradiction. Thus since λ_n was chosen arbitrary, we arrived at (as $b_\lambda = 1/a_\lambda$)) $a_{\lambda=1^-} = \lim_{\lambda\to 1^-} a_\lambda = 0^+$ and $b_{\lambda=1^-} = \lim_{\lambda\to 1^-} b_\lambda = +\infty$. A simple inspection of (14) shows that $a_{\lambda=0} = \sqrt{2} - 1$ and $b_{\lambda=0} = (1/(\sqrt{2}-1)) = 1 + \sqrt{2}$. In addition as proved above $a_{\lambda=1^-} = 0^+$ and $b_{\lambda=1^-} = +\infty$.

Hence $x_0 \in (a_{\lambda_0}, b_{\lambda_0})$ ensures that $x_0 \in (a_\lambda, b_\lambda)$ for all $[\lambda_0, 1)$. The latter in fact follows for all $\lambda \in [\lambda_0, 1]$ as the case of $\lambda = 1$ always renders ψ a reparameterization (see [8] or [14]).

A particular candidate for λ_0 can be found e.g. upon inspecting *a look-up Table 1*. In order to accept vaster class of admissible exponential parameterizations yielding ψ as a reparameterization, the look-up table, should in practice contain the intervals (a_λ, b_λ) computed for a denser increment of $\lambda \in [0, 1)$, preferably equal to 0.01. This can be achieved by extending Table 1 to more entries upon again invoking *Mathematica* package.

Recall that more-or-less uniform samplings (2) satisfy $\beta \leq x = N_{im}/M_{im} \leq (1/\beta)$. Consequently, given the β is known a priori, if both inequalities $\beta > a_{\lambda_0}$ and $(1/\beta) < b_{\lambda_0}$ hold, then ψ is asymptotically a reparametrization for all $\lambda \in [\lambda_0, 1)$ (and also for $\lambda \in [\lambda_0, 1]$). In particular, if $\beta > a_{\lambda=0} = \sqrt{2} - 1$ and $(1/\beta) < b_{\lambda=0} = \sqrt{2} + 1$, which both hold for $\beta > \sqrt{2} - 1$, then ψ defines a genuine piecewise C^∞ reparameterization for each $\lambda \in [0, 1]$ defining (3). For such more-or-less uniform samplings no support of the look-up table is required.

b) Alternatively (to get more geometrical insight into (13)), for any fixed $\lambda \in [0, 1)$ one solves both inequalities from (11) over the domain $[0, 1] \times [0, 1]$ with the aid of symbolic computation (i.e. with the *Mathematica RegionPlot* function). The geometrical plots of *2D admissible zone* A_λ (see e.g. shaded areas

Table 1. Numerically computed admissible intervals (a_λ, b_λ) for various $\lambda \in [0,1)$

$\lambda = 0.0$	$\lambda = 0.1$	$\lambda = 0.2$	$\lambda = 0.3$	$\lambda = 0.4$
(0.414,2.414)	(0,381,2.622)	(0.345,2,901)	(0.304,3.294)	(0.257,3.885)
$\lambda = 0.5$	$\lambda = 0.6$	$\lambda = 0.7$	$\lambda = 0.8$	$\lambda = 0.9$
(0.216,4.865)	(0.148,6.761)	(0.086, 11.599)	(0.029,34.394)	(0.001,1028.990)

in Fig. 2) admits any sampling pairs $(x, y) = (M_{im}, N_{im}) \in A_\lambda$, for different $\lambda \in [0,1]$ rendering ψ_i asymptotically a reparameterization. Note that for arbitrary more-or-less uniform samplings (and any fixed $\lambda \in [0,1)$ in exponential parameterization (3)) an admissible zone for (M_{im}, N_{im}) is in fact a sub-square $[\beta, 1]^2 \subset [0,1]^2$, where $0 < \beta \leq 1$ is defined as in (2). A straightforward verification shows that for $\lambda = 1$ both equations in (11) are satisfied and therefore $A_1 = [0,1] \times [0,1]$. The case when $\lambda = 0$ reduces (11) into $\frac{1}{x} - \frac{x}{x+y}\left(\frac{1}{y} - \frac{1}{x}\right) > 0$ and $\frac{1}{y} + \left(1 + \frac{x}{x+y}\right)\left(\frac{1}{y} - \frac{1}{x}\right) > 0$, which in turn become $y^2 - x^2 + 2xy > 0$ and $x^2 - y^2 + 2xy > 0$, thus yielding $A_0 = \{(x,y) \in [0,1]^2 : y > (\sqrt{2}-1)x, y < (1/(\sqrt{2}-1))x = (\sqrt{2}+1)x\}$. The latter corresponds to a_0 and b_0 computed above. The symmetry of A_λ for other $\lambda \in (0,1)$ with respect to line $y = x$ (as expected due to $a_\lambda = (1/b_\lambda)$) is illustrated in Figure 2 for $\lambda \in \{0, 0.5, 0.7\}$. Noticeably symbolic computation by *RegionPlot* shows that $A_{\lambda_1} \subset A_{\lambda_2}$ for $\lambda_1 < \lambda_2$, where $\lambda_i \in [0,1]$. The latter follows also independently from (15).

Since for samplings (2) we have $\beta \leq (x/y) \leq (1/\beta)$ and $\beta \leq (y/x) \leq (1/\beta)$, the pair (M_{im}, N_{im}) belongs to the set $B = \{(x,y) \in [0,1]^2 : y \leq \beta^{-1}x, y \geq \beta x\}$. Hence if $B \subset A_{\lambda_0}$ then $B \subset A_\lambda$, for all $\lambda \in [\lambda_0, 1]$. This renders ψ asymptotically a piecewise C^∞ reparameteriztion for all $\lambda \in [\lambda_0, 1]$. In particular, the latter holds for all $\lambda \in [0,1]$ given $B \subset A_0$ (since then $A_0 \subset A_\lambda$). □

Unfortunately, the verification of condition (12) is harder and each time demands an extra analysis. To circumvent this difficulty, a stronger condition guaranteeing the fulfillment of both (11) and (12) is proposed below. More precisely, one assumes here the existence of two positive number (σ_1, σ_2) independent on

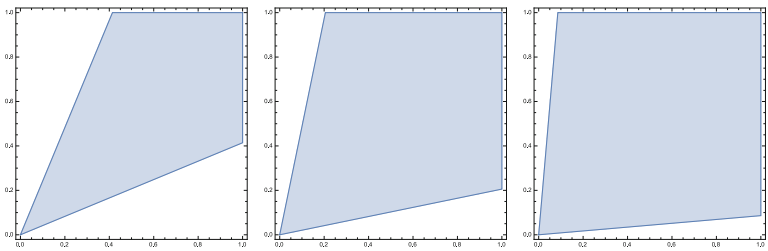

a) b) c)

Fig. 2. The plots of 2D admissible zones A_λ, for: a) $\lambda = 0$, b) $\lambda = 0.5$ and c) $\lambda = 0.7$

m, i and $\lambda \in [\lambda_0, 1]$ satisfying the following two inequalities (at least asymptotically):

$$\rho_1(M_{im}, N_{im}) \geq \sigma_1 > 0 \quad \text{and} \quad \rho_2(M_{im}, N_{im}) \geq \sigma_2 > 0. \tag{16}$$

Evidently, the satisfaction of (16) implies that (11) and (12) hold which in turn yields ψ_i as a reparameterization for $\lambda \in [\lambda_0, 1]$. Geometrically, any pair of $\sigma = (\sigma_1, \sigma_2)$ introduces an extra buffer zone in corrected 2D admissible regions A^{σ}_{λ} this time by making the left-hand sides in (11) stay away from zero, which is enforced by (16). The practical procedure to determine whether ψ_i indeed is a reparameterization relies on fixing $\sigma = (\sigma_1, \sigma_2)$ and performing *Mathematica* symbolic calculation with *RegionPlot* function to plot A^{σ}_{λ} for incremented λ. If there exists λ_0 such that a given family of more-or-less uniform samplings satisfies $(M_{im}, N_{im}) \in A^{\sigma}_{\lambda}$ for all $\lambda \in [\lambda_0, 1]$, then condition (16) follows. One can also vary σ and repeat the above procedure in a search for smaller value of λ_0.

The mathematical argument to solve (13) is extendable to (16) (with $\sigma = \sigma_1 = \sigma_2$) if extra assumptions on samplings $\mathcal{T}_m$ are made. This ultimately leads to the shifted inequalities $f(x) > g(x) + \sigma$ and $g(x) - \sigma > h(x)$ similar to those already discussed from (14). However, the latter exceeds the scope of this paper.

4 Experiments

The tests are conducted in *Mathematica 9.0* (see [17]) on a 2.4GHZ Intel Core 2 Duo computer with 8GB RAM. Note that since $T = \sum_{i=1}^{m}(t_{i+1} - t_i) \leq m\delta_m$ the following holds $m^{-\alpha} = O(\delta_m^{\alpha})$ for $\alpha > 0$. Hence, the verification of the asymptotics expressed in terms of $O(\delta_m^{\alpha})$ can be examined in terms of $O(1/m^{\alpha})$ asymptotics. For a regular curve $\gamma : [0, T] \to E^n$, $\lambda \in [0, 1]$ and m varying between $m_{min} \leq m \leq m_{max}$, the error for γ estimation over $[t_i, t_{i+2}]$ reads

$$E^i_m = \sup_{t \in [t_i, t_{i+2}]} \|(\hat{\gamma}_{2,i} \circ \psi_i)(t) - \gamma(t)\| = max_{t \in [t_i, t_{i+2}]} \|(\hat{\gamma}_{2,i} \circ \psi_i)(t) - \gamma(t)\|, \tag{17}$$

as $\tilde{E}^i_m(t) = \|(\hat{\gamma}_{2,i} \circ \psi_i)(t) - \gamma(t)\| \geq 0$ is continuous over each sub-interval $[t_i, t_{i+2}] \subset [0, T]$. The maximal value E_m of $\tilde{E}_m(t)$ (the track-sum of $\tilde{E}^i_m(t)$), for each $m = 2k$ (here $k = 1, 2, 3, \ldots, m/2$) is found by using *Mathematica* optimization built-in functions *Maximize* or *FindMinimum* (the latter applied to $-\tilde{E}_m(t)$). Since $deg(\hat{\gamma}_2) = 2$, the number of interpolation points $\{q_i\}_{i=0}^{m}$ is odd i.e. $m = 2k$. The *Mathematica* built-in functions *LinearModelFit* calculates the coefficient $\bar{\alpha}(\lambda)$ from the computed regression line $y(x) = \bar{\alpha}(\lambda)x + b$ on pairs of points $\{(\log(m), -\log(E_m))\}_{m=m_{min}}^{m_{max}}$ (see [7]). In order to test that ψ_i is asymptotically a parameterization (for a fixed $\lambda \in [0, 1)$), it suffices to show that both constraints $(M_{im}/N_{im}) \in (a_\lambda, b_\lambda)$ and (12) are fulfilled for sufficiently large m. Recall that, the second condition can be replaced by a stronger one formulated in (16). In the event of difficulties in verification of the above two conditions, one may test in practice (for large $m = m_{max}$) both inequalities $\psi_i^{(1)}(t_i) > 0$

and $\psi_i^{(1)}(t_{i+2}) > 0$ which should hold over each sub-interval $[t_i, t_{i+2}]$. Evidently, such an approach only partially alleviates the problem, as it relies on the implicit assumption that both inequalities hold asymptotically i.e. for sufficiently large m. The next two examples confirm numerically the sharpness of Th. 3 and illustrate our procedure designed to determine when ψ is a piecewise C^∞ parameterization.

Example 1. Let a regular spatial curve in E^3 be *a quadratic elliptical helix*:

$$\gamma_h(t) = (2\cos(t), \sin(t), t^2), \tag{18}$$

with $t \in [0, 2\pi]$, be sampled more-or-less uniformly (2) (with $\beta = (1/3)$) as:

$$t_i = \begin{cases} \frac{2\pi i}{m} & \text{if } i \text{ even}, \\ \frac{2\pi i}{m} + \frac{\pi}{m} & \text{if } i = 4k+1, \\ \frac{2\pi i}{m} - \frac{\pi}{m} & \text{if } i = 4k+3. \end{cases} \tag{19}$$

Figure 3 shows a plot of γ_h sampled in accordance with (19) for $m = 22$. Note that here $\delta_m = (3\pi/m)$ and over each segment $[t_i, t_{i+2}]$ we either have $t_{i+1} - t_i = \delta_m$ and $t_{i+2} - t_{i+1} = (1/3)\delta_m$ or $t_{i+1} - t_i = (1/3)\delta_m$ and $t_{i+2} - t_{i+1} = \delta_m$. This results only in two pairs $(M_1, N_1) = (1, 1/3)$ and $(M_2, N_2) = (1/3, 1)$ which are independent of m. The inequality $\beta = (1/3) > \sqrt{2} - 1$ from Th. 4 does not hold and thus the look-up Table 1 is used which yields $(N_1/M_1) = (1/3) \in (a_{0.3}, b_{0.3}) = (0.304, 3.294)$ and $(N_2/M_2) = 3 \in (a_{0.3}, b_{0.3})$. Thus (11) holds for all $\lambda \in [0.3, 1)$. In fact there exists exactly one $\lambda_e \approx 0.3$ such that for all $\lambda \in [\lambda_e, 1)$ all intervals (a_λ, b_λ) are admissible. To test the first condition in (12) we solve (with respect to λ) two equations $\rho_1(M_1, N_1) = 0$ and $\rho_1(M_2, N_2) = 0$. Indeed, for $\rho_1(M_1, N_1) = 0$ we have

$$1^{\lambda-1} - \frac{1}{1+\frac{1}{3}}\left(\left(\frac{1}{3}\right)^{\lambda-1} - 1^{\lambda-1}\right) = 0 \equiv \left(\frac{7}{9}\right) = \left(\frac{1}{3}\right)^{\lambda}.$$

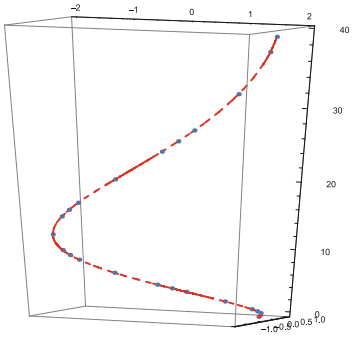

Fig. 3. The plot of the hellix γ_h from (18) sampled according to (19), for $m = 22$

The latter separates $\lambda_e = \frac{\ln(9)-\ln(7)}{\ln(3)} \approx 0.2287$ from the admissible interval $[0.3, 1)$ while $m \to \infty$. Similarly, for $\rho_1(M_2, N_2) = 0$ we obtain

$$\left(\frac{1}{3}\right)^{\lambda-1} - \frac{\frac{1}{3}}{\frac{1}{3}+1}\left(1^{\lambda-1} - \left(\frac{1}{3}\right)^{\lambda-1}\right) = 0 \equiv \left(\frac{1}{15}\right) = \left(\frac{1}{3}\right)^{\lambda}.$$

This gives another $\lambda_e = \frac{\ln(15)}{\ln(3)} \approx 2.465 \notin [0, 1)$ separated from $[0.3, 1)$, while $m \to \infty$. Similarly, $\rho_2(M_1, N_1) = 0$ becomes

$$1^{\lambda-1} + \left(1 + \frac{\frac{1}{3}}{1+\frac{1}{3}}\right)\left(\left(\frac{1}{3}\right)^{\lambda-1} - 1^{\lambda-1}\right) = 0 \equiv \left(\frac{1}{15}\right) = \left(\frac{1}{3}\right)^{\lambda}.$$

As previously, $\lambda_e \approx 2.465 \notin [0, 1)$ and also is separated from $[0.3, 1)$ for $m \to \infty$. Finally, $\rho_2(M_2, N_2) = 0$ transforms into:

$$\left(\frac{1}{3}\right)^{\lambda-1} + \left(1 + \frac{1}{1+\frac{1}{3}}\right)\left(1^{\lambda-1} - \left(\frac{1}{3}\right)^{\lambda-1}\right) = 0 \equiv \left(\frac{7}{9}\right) = \left(\frac{1}{3}\right)^{\lambda}.$$

Similarly, $\lambda_e \approx 0.2287 \in [0, 1)$ is separated from $[0.3, 1)$, while $m \to \infty$. As both ρ_1 and ρ_2 are continuous over $(M_{im}, N_{im}) \in [\beta, 1] \times [\beta, 1]$, a small separation of (11) away from zero by introducing $\sigma = (\sigma_1, \sigma_2)$ (see (16)) should still keep the shifted λ_e^{σ} away from $[0.3, 1)$. This is illustrated in Fig. 4 with the aid of *RegionPlot* function visualizing 2D admissible zone $A_{0.3}$ against the buffer admissible zones A_{λ}^{σ}, with $\sigma_1 = \sigma_2 = 0.01$ and $\lambda \in \{0.3, 0.5, 0.7, 08\}$. Note that similarly to A_{λ} we also have $A_{\lambda_1}^{\sigma} \subset A_{\lambda_1}^{\sigma}$ for $\lambda_2 > \lambda_1$.

A linear regression to approximate $\alpha(\lambda)$ is used here with $m_{min} = 101 \leq m \leq m_{max} = 121$. The computed estimates $\bar{\alpha}(\lambda) \approx \alpha(\lambda)$ for various $\lambda \in [0, 1]$ are shown in Table 2. Visibly the sharpness of Th. 3 is experimentally confirmed. Note that the asymptotics established in Th. 3 holds for any $\lambda \in [0, 1]$ without actually assuming ψ_i to be a reparameterization. However, the latter is vital in approximating length of γ or if one-two-one local correspondence between interpolant $\hat{\gamma}_2$ and the curve γ is required. □

Table 2. Estimated $\bar{\alpha}(\lambda) \approx \alpha(\lambda)$, for γ_h and (19) interpolated by $\hat{\gamma}_2$ with $\lambda \in [0, 1]$

$\lambda = 0.00$	$\lambda = 0.10$	$\lambda = 0.33$	$\lambda = 0.50$	$\lambda = 0.70$	$\lambda = 0.90$	$\lambda = 1.00$
1.001	1.000	1.001	0.999	1.001	1.058	2.931

Example 2. Consider *a planar regular convex spiral* $\gamma_{sp} : [0, 5\pi] \to E^2$

$$\gamma_{sp}(t) = ((6\pi - t)\cos(t), (6\pi - t)\sin(t)) \tag{20}$$

sampled first as in (19). Figure 5 a) illustrates the curve γ_{sp} sampled along (19) with Q_{22}. Evidently, the same conclusion as reached in the last example,

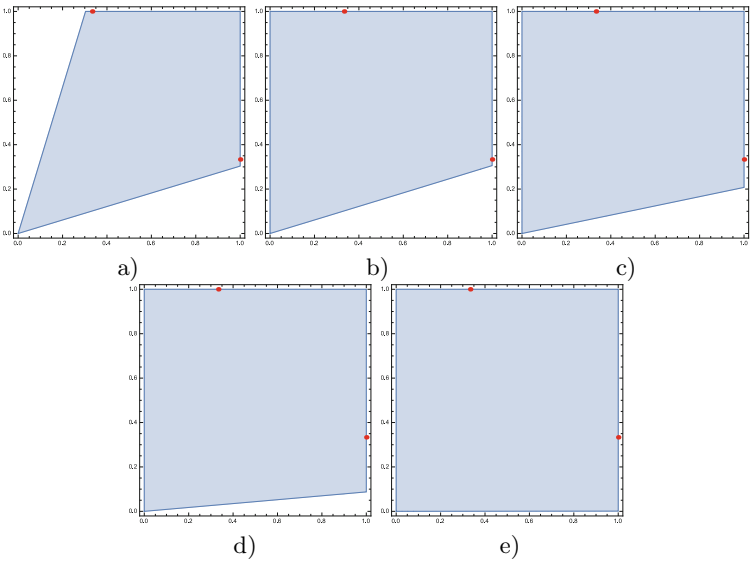

Fig. 4. The plots of admissible zones: a) $A_{0.3}$ b)-e) buffer $A_{\lambda}^{0.01}$ for $\lambda \in \{0.3, 0.5, 0.7, 0.9\}$ all containing samplings (19) (represented by two red dots)

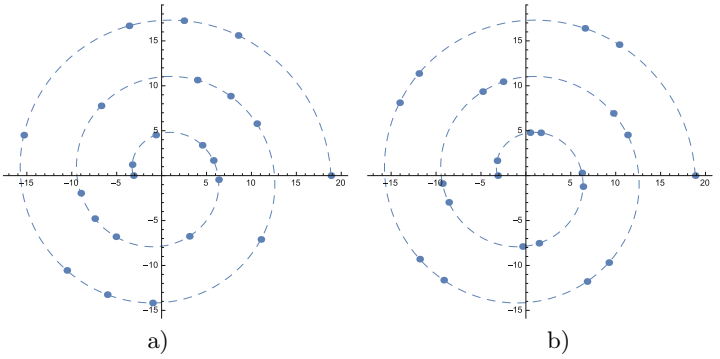

Fig. 5. The plot of γ_{sp} from (20) sampled according to: a) (19) and b) (21), for $m = 22$

Table 3. Estimated $\bar{\alpha}(\lambda) \approx \alpha(\lambda) = 1$ for γ_{sp} and (19) interpolated by $\hat{\gamma}_2$ with $\lambda \in [0, 1]$

$\lambda = 0.00$	$\lambda = 0.10$	$\lambda = 0.33$	$\lambda = 0.50$	$\lambda = 0.70$	$\lambda = 0.90$	$\lambda = 1.00$
0.980	0.982	1.012	1.021	1.009	1.619	2.997

applies here as it merely depends on specific sampling and λ. For the numerical approximation of $\alpha(\lambda)$ a linear regression is used with $101 \leq m \leq 121$. The results from Table 3 confirm sharpness of the asymptotics established in Th. 3.

Finally, we admit another more-or-less uniform sampling (2) (where $\beta = (1/5)$):

$$t_i = \frac{5\pi i}{m} + \frac{(-1)^{i+1}5\pi}{3m}, \tag{21}$$

with $t_0 = 0$ and $t_m = 5\pi$ - see Figure 5 b). The generic sub-interval $[t_i, t_{i+2}]$ (with i even) yields $t_{i+1} - t_i = \frac{5\cdot 5\pi}{3m} = 1 \cdot \delta_m$ and $t_{i+2} - t_{i+1} = \frac{5\pi}{3m} = \frac{1}{5}\delta_m$. Thus $(M_{im}, N_{im}) = (1, \frac{1}{5})$ and therefore $(N_{im}/M_{im}) = (1/5) \in (a_{0.6}, b_{0.6}) = (0.148, 6.761)$ - see Table 1. Thus condition (11) holds for $\lambda \in [0.6, 1)$.

Note that if a look-up table resolution on λ is increased, then a better estimate of λ_0 can be obtained. As in Example 1, one searches now for λ enforcing $\rho_1(1, (1/5)) = 0$ and $\rho_2(1, (1/5)) = 0$. In doing so, we first obtain

$$1^{\lambda-1} - \frac{1}{1+\frac{1}{5}}\left(\left(\frac{1}{5}\right)^{\lambda-1} - 1^{\lambda-1}\right) = 0 \equiv \left(\frac{9}{20}\right) = \left(\frac{1}{5}\right)^{\lambda}.$$

Hence $\lambda_e = \frac{\ln(20)-\ln(9)}{\ln(5)} \approx 0.4961 \in [0, 1)$ is separated from $[0.6, 1)$ for $m \to \infty$. Similarly, $\rho_2(1, (1/5)) = 0$ amounts to

$$1^{\lambda-1} + \left(1 + \frac{\frac{1}{5}}{1+\frac{1}{5}}\right)\left(\left(\frac{1}{5}\right)^{\lambda-1} - 1^{\lambda-1}\right) = 0 \equiv \left(\frac{1}{35}\right) = \left(\frac{1}{5}\right)^{\lambda}.$$

The latter gives $\lambda_e = \frac{\ln(35)}{\ln(5)} \approx 2.2090 \notin [0, 1)$ which is separated from $[0.6, 1)$ when $m \to \infty$. Again, as both ρ_1 and ρ_2 are continuous over $(M_{im}, N_{im}) \in [\beta, 1] \times [\beta, 1]$ a small separation of (11) away from zero by introducing $\sigma = (\sigma_1, \sigma_2)$ (see (16)) should still keep the shifted λ_e^{σ} away from $[0.6, 1)$. This effect is illustrated with the aid *RegionPlot* function to visualize 2D admissible zone $A_{0.6}$ against buffer admissible zones A_{λ}^{σ}, with $\sigma_1 = \sigma_2 = 0.01$ and different $\lambda \in \{0.6, 0.7, 0.8, 0.9\}$. Again, as in the case of A_{λ}, we have $A_{\lambda_1}^{\sigma} \subset A_{\lambda_2}^{\sigma}$ for $\lambda_1 < \lambda_2$.

For the numerical approximation of $\alpha(\lambda)$ a linear regression is used again with $101 \leq m \leq 121$. Table 4 contains numerical estimates of $\alpha(\lambda) = 1$ for various $\lambda \in [0, 1)$. Visibly the results confirm the sharpness of the asymptptics derived in Th. 3. □

Table 4. Estimated $\bar{\alpha}(\lambda, 0) \approx \alpha(\lambda, 0) = 1$ (with $\lambda \in [0, 1)$) and $\bar{\alpha}(1, 0) \approx \alpha(1, 0) = 3$ for γ_{sp} and sampling (21) interpolated by $\hat{\gamma}_2$ with $\lambda \in [0, 1]$

$\lambda = 0.00$	$\lambda = 0.10$	$\lambda = 0.33$	$\lambda = 0.50$	$\lambda = 0.70$	$\lambda = 0.90$	$\lambda = 1.00$
0.990	0.990	0.991	0.998	1.020	1.320	3.000

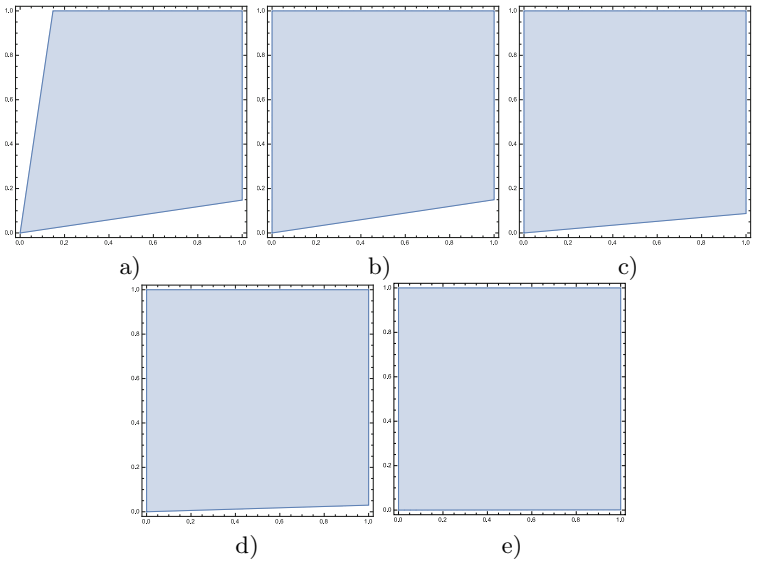

Fig. 6. The plots of admissible zones: a) $A_{0.6}$ b)-e) buffer $A_{\lambda}^{0.01}$ for $\lambda \in \{0.6, 0.7, 0.8, 0.9\}$ all containing samplings (21) (represented by single red dot)

5 Conclusions

This work supplements Th. 3 (see [8]) concerning the asymptotics in trajectory estimation via piecewise-quadratic interpolation $\hat{\gamma}_2 : [0, \hat{T}] \to E^n$ based on reduced data Q_m and exponential parameterization (3). The curve $\gamma : [0, T] \to E^n$ is assumed to be sampled more-or-less uniformly (2) for $\lambda \in [0, 1)$ and sampled along (1) for $\lambda = 1$. Th. 3 assumes the existence of a reparameterization $\psi : [0, T] \to [0, \hat{T}]$ between γ and $\hat{\gamma}_2$. This paper formulates sufficient conditions imposed on samplings (2) and $\lambda \in [0, 1)$ to guarantee that $\dot{\psi} > 0$ - see Th. 4 and (16). Recall that for $\lambda = 1$, a quadratic ψ defines a reparameterization (see [8]). The analysis performed here and the accompanying procedure is supported by the geometrical insight, symbolic computation and numerical verification of both Th. 3 and Th. 4. A possible extension of this work is to invoke smooth interpolation schemes (see [1]) combined with reduced data and exponential parameterization (see [11]). Certain clues may be found in [4], where complete C^2 splines [1] are dealt with $\lambda = 1$ to establish the fourth orders of convergence in trajectory and length estimation. In general for length estimation (as well as for the genuine trajectory tracking) the mapping ψ needs to be a reparameterization (see also [7]). The analysis of C^1 interpolation for reduced data with cumulative chords can be found in [7] or [9]. Some applications and theory on non-parametric interpolation can be found e.g., in [11], [7] or [5]. Related work on other knots' parameterizations are discussed in [11], [12], [6], [13] and [2]. Finally, we should point out that one can also consider the other subfamilies of admissible samplings (1) different than more-or-less uniform (2). One of them

introduces so-called ε-uniform samplings (see e.g. [15]). Recent result [10] shows (among all) that for such samplings combined with reduced data Q_m and exponential parametrization (3), the quadratic ψ used in proving Th. 4 defines a genuine piecewise C^∞ reparameterization for each $\lambda \in [0,1]$). In addition, the latter yields faster convergence orders in $\hat{\gamma}_2 \circ \psi - \gamma$ as opposed to those in Th. 3.

References

1. de Boor, C.: A Practical Guide to Splines. Springer-Verlag, Heidelberg (2001)
2. Epstein, M.P.: On the influence of parameterization in parametric interpolation. SIAM Journal of Numerical Analysis **13**, 261–268 (1976)
3. Farin, G.: Curves and Surfaces for Computer Aided Geometric Design, 3rd edn. Academic Press, San Diego (1993)
4. Floater, M.S.: Chordal cubic spline interpolation is fourth order accurate. IMA Journal of Numerical Analysis **26**, 25–33 (2006)
5. Janik, M., Kozera, R., Kozioł, P.: Reduced data for curve modeling - applications in graphics, computer vision and physics. Advances in Science and Technology **7**(18), 28–35 (2013)
6. Kocić, L.M., Simoncelli, A.C., Della Vecchia, B.: Blending parameterization of polynomial and spline interpolants, Facta Universitatis (NIŠ). Series Mathematics and Informatics **5**, 95–107 (1990)
7. Kozera, R.: Curve modeling via interpolation based on multidimensional reduced data. Studia Informatica **25**(4B–61), 1–140 (2004)
8. Kozera, R., Noakes, L.: Piecewise-quadratics and exponential parameterezіation for reduced data. Applied Mathematics and Computaion **221**, 1–19 (2013)
9. Kozera, R., Noakes, L.: C^1 interpolation with cumulative chord cubics. Fundamenta Informaticae **61**(3–4), 285–301 (2004)
10. Kozera, R., Noakes, L.: Exponential parameterization and ε-uniformly sampled reduced data. Applied Mathematics and Information Sciences. Accepted for publication
11. Kvasov, B.I.: Methods of Shape-Preserving Spline Approximation. World Scientific Publishing Company, Singapore (2000)
12. Lee, E.T.Y.: Choosing nodes in parametric curve interpolation. Computer-Aided Design **21**(6), 363–370 (1989)
13. Mørken, K., Scherer, K.: A general framework for high-accuracy parametric interpolation. Mathematics of Computaion **66**(217), 237–260 (1997)
14. Noakes, L., Kozera, R.: Cumulative chords piecewise-quadratics and piecewise-cubics. In: Klette, R., Kozera, R., Noakes, L., Weickert, J. (eds.) Geometric Properties of Incomplete Data, Computational Imaging and Vision, vol. 31, pp. 59–75. Kluver Academic Publishers, The Netherlands (2006)
15. Noakes, L., Kozera, R., Klette, R.: Length estimation for curves with different samplings. In: Bertrand, G., Imiya, A., Klette, R. (eds.) Digital and Image Geometry. LNCS, vol. 2243, pp. 339–351. Springer, Heidelberg (2002)
16. Piegl, L., Tiller, W.: The NURBS Book. Springer-Verlag, Heidelberg (1997)
17. Wolfram Mathematica 9, Documentation Center. `http://reference.wolfram.com/mathematica/guide/Mathematica.html`